Photoinduced intermolecular electron transfer in complex liquids: Experiment and theory

H. L. Tavernier, M. M. Kalashnikov, and M. D. Fayer[a)]
Department of Chemistry, Stanford University, Stanford, California 94305

(Received 2 August 2000; accepted 18 September 2000)

Photoinduced intermolecular electron transfer between Rhodamine 3B and *N*,*N*-dimethylaniline has been studied in a series of seven liquids: acetonitrile, ethanol, propylene glycol, and mixtures of ethanol, 2-butanol, ethylene glycol, propylene glycol, and glycerol. In each liquid, the donor and acceptors have different diffusion constants and experience distinct dielectric properties. Ps time-dependent fluorescence measurements and steady-state fluorescence yield measurements were made and analyzed using a detailed statistical mechanical theory that includes a distance-dependent Marcus rate constant, diffusion with the hydrodynamic effect, and solvent structure. All solvent-dependent parameters necessary for calculations were measured, including dielectric constants, diffusion constants, and redox potentials, leaving the electronic coupling unknown. Taking the distance-dependence of the coupling to be $\beta = 1\ \text{Å}^{-1}$, data were fit to a single parameter, the coupling matrix element at contact, J_0. The theory is able to reproduce both the functional form of the time-dependence and the concentration-dependence of the data in all seven liquids by fitting only J_0. Despite the substantial differences in the properties of the experimental systems studied, fits to the data are very good and the values for J_0 are very similar for all solvents. © *2000 American Institute of Physics.* [S0021-9606(00)01846-8]

I. INTRODUCTION

Electron transfer reactions in liquids are dependent on the properties of the donor/acceptor molecules themselves and on the properties of the liquid solvent. For example, solvent dielectric properties affect free energies of transfer and solvation energies. In heterogeneous media, dielectric properties of nearby structures can affect electron transfer.[1–3] Intermolecular electron transfer in solution has the added complexity of donor–acceptor distance distributions and diffusion of the species. Both the distance distribution, which is determined by the radial distribution function, and the rates of diffusion are linked to the specific properties of the solvent.

Numerous studies have been performed addressing the dependence of electron transfer on environments including liquids,[4–7] micelles,[1,8–11] vesicles,[12] proteins,[13–15] and DNA.[2,16–19] It is often difficult to analyze experimental intermolecular electron transfer data due to the complexity of the systems. Some system properties that affect electron transfer can be measured; these include solvent dielectric constants, redox potentials, and bulk diffusion constants. Some factors, like a distance-dependent transfer rate, distance-dependent diffusion, and solvent structure can be described theoretically and therefore must be included in calculations of electron transfer dynamics to obtain a proper description of the dynamics.

In this paper, time dependent fluorescence data and steady state fluorescence yield data are used to examine photoinduced electron transfer for donors and acceptors in seven liquid solvents. Rhodamine 3B (R3B), in low concentration, is photo-excited. It is the hole donor. *N*,*N*-dimethylaniline (DMA), in various high concentrations, is the hole acceptor. Acetonitrile was chosen as an exemplary nonhydrogen-bonding solvent. Measurements were performed in ethanol and propylene glycol as examples of pure hydrogen-bonding solvents. In addition, data were taken in four alcohol mixtures. Studying electron transfer in such a diverse collection of solvents yields important information about electron transfer dynamics, solvent effects, and ability of theory to successfully describe the data.

The data were analyzed with an analytical, statistical mechanical theory that encompasses a number of key elements that affect photoinduced intermolecular electron transfer.[20–23] The theory can be used to calculate electron transfer observables and includes the effects of solvent structure and diffusion with the hydrodynamic effect. A Marcus distance-dependent transfer rate is used to describe through-solvent transfer and incorporates solvent dielectric constants, redox potentials, excitation energies, and Coulomb interactions. The theory also includes solvent structure, which determines the donor–acceptor radial distribution function, and the hydrodynamic effect, that is, the distance dependence of the diffusion constant, because these factors can have a significant effect on electron transfer. All parameters necessary for the data analysis were measured or calculated, with the exception of the donor–acceptor electronic coupling parameters. Measurements were made of the solvent dielectric constants, the donor/acceptor diffusion constants in each solvent, and the donor/acceptor redox potentials. In addition, the radial distribution functions and the hydrodynamic effects were calculated for each solvent. Fits to electronic coupling parameters yield remarkably similar results for all solvents.

[a)]Author to whom correspondence should be addressed. Electronic mail: fayer@fayerlab.stanford.edu; Fax: (650) 723-4817

II. EXPERIMENTAL PROCEDURES

A. Sample preparation

Samples were prepared in the following seven solvents: acetonitrile, ethanol, propylene glycol (1,2-propanediol), 58/42 v/v propylene glycol/2-butanol, 23/77 v/v glycerol/2-butanol, 50/50 v/v ethylene glycol/ethanol, and 41/59 v/v glycerol/ethanol. All solvents were the highest grade commercially available and were used as received. 2-butanol was used in some of the mixtures because its size is similar to that of propylene glycol and glycerol, and it is easier to describe the solvent structure of a mixture whose components have similar sizes. The solvent ratios used in glycerol/ethanol, glycerol/2-butanol, and propylene glycol/2-butanol mixtures were chosen so that they would have similar viscosities. However, measurements of the diffusion constants showed that similarity in viscosity did not produce similar diffusion constants.

Each sample contained ~0.04 mM Rhodamine 3B perchlorate (R3B, Exciton), the photoexcited hole donor. Rhodamine 3B is the ethyl ester of Rhodamine B. For each solvent, one sample was prepared with only R3B and 3 samples were prepared with different concentrations of the hole acceptor, *N*,*N*-dimethylaniline (DMA, Aldrich, packaged under nitrogen). DMA concentrations ranged from 0.025 M to 0.15 M.

B. Fluorescence experiments

Both time-resolved and steady-state fluorescence measurements were performed using a mode-locked, Q-switched Nd:YLF laser. Frequency-doubled YLF pulses pumped two cavity-dumped dye lasers. A Rhodamine 6G (Exciton) dye laser was tuned to 572 nm to excite at the red side of the Rhodamine 3B absorption spectrum. The second dye laser used LDS 867 (Exciton) to achieve 880 nm pulses. Pulse lengths were ~35 ps. Time-resolved fluorescence was measured by fluorescence up-conversion. Fluorescence was summed with the 880 nm pulses in a RDP crystal. The up-converting beam polarization was at the magic angle with respect to the excitation beam. The intensity of the up-conversion signal was detected with a dry ice-cooled PMT. Steady-state fluorescence was detected at the magic angle with a PMT. Experiments were performed at room temperature.

C. Diffusion constant and redox potential measurements

Both bulk diffusion constants and reduction/oxidation potentials of the donor/acceptor molecules were measured at room temperature by cyclic voltammetry. Measurements were made with an Ensman Instruments EI 400 dual-electrode potentiostat in two-electrode mode. The working electrode was a Bioanalytical Systems 10 μm diameter Pt ultramicroelectrode and the reference electrode was $Ag/AgNO_3$ with tetrabutylammonium perchlorate (TBAP) or tetrahexylammonium perchlorate (THAP) in acetonitrile or 2-propanol. All measurements were made from steady-state sigmoidal voltammograms with a scan rate of 10 mV/s. Approximately 0.1 M TBAP or THAP was used as the electrolyte for each measurement. The solutions were bubbled vigorously with N_2 for 15 min prior to all R3B measurements. DMA concentrations used were 0.03–0.2 mM and R3B concentrations were 0.1–2 mM.

The difference between DMA oxidation and R3B reduction potentials, $\Delta E^0 = E^0_{\mathrm{DMA,ox}} - E^0_{\mathrm{R3B,red}}$, was measured with DMA and R3B both in the same THAP/acetonitrile solution. For acetonitrile, which has a dielectric constant of $\epsilon_{\mathrm{st}} = 35.9$,[24] $\Delta E^0_{\epsilon_{\mathrm{st}}=35.9} = 1.55 \pm 0.06$ eV. Redox potentials are corrected for dielectric constant in each solvent according to the following equation:[1,25,26]

$$\Delta E^0 = \Delta E^0_{\epsilon_{\mathrm{st}}=35.9} + \frac{e^2}{8\pi\epsilon_0}\left(\frac{1}{\epsilon_{\mathrm{st}}} - \frac{1}{35.9}\right)\left(\frac{1}{r_a} - \frac{1}{r_d}\right), \qquad (1)$$

where e is the charge of an electron, ϵ_0 is the permittivity of free space, ϵ_{st} is the solvent dielectric constant, and $r_{a/d}$ are the acceptor/donor radii. The corrections were small. The maximum correction is 0.02 eV, for the glycerol/2-butanol mixture.

Diffusion constants were calculated from the measured limiting current, i_l,[27]

$$i_l = 4nFDcr_e, \qquad (2)$$

where n is the number of electrons transferred per molecule, F is Faraday's constant, D is the bulk diffusion constant, c is the bulk concentration of the electroactive species, and r_e is the electrode radius. The electrode radius was calibrated using ferrocene in acetonitrile to get $D = 21.7 \times 10^{-6}$ cm^2/s.[27] Limiting currents were measured for DMA in all solvents. Because measurement of the R3B limiting current was so difficult, it was only measured in acetonitrile, ethanol, ethanol/ethylene glycol, and glycerol/ethanol. Measurement errors were $\pm 10\%$ for DMA and $\pm 20\%$ for R3B. Diffusion constants for R3B in other solvents were calculated by multiplying the measured value in ethanol by the ratio of solvent viscosities ($\eta_{\mathrm{ethanol}}/\eta_{\mathrm{other}}$), in accordance with the Stokes–Einstein equation. Diffusion constants are listed in Table I. The mutual diffusion constant (the sum of the donor and acceptor diffusion constants) was used in calculations. Because DMA is substantially smaller than R3B, it dominates the mutual diffusion constant, reducing the significance of the error in the R3B measurements.

The viscosity of each solvent was measured using a series of Cannon Ubbelohde viscometers. Viscosities (η) are reported in Table I.

D. Dielectric constant measurements

The index of refraction of each solvent was measured at room temperature using a refractometer. Optical dielectric constants (ϵ_{op}), reported in Table II, are the square of the refractive index.

Static dielectric constants (ϵ_{st}) were measured at room temperature using a concentric cylinder capacitor. The solvent was held in a graduated cylinder. A stainless steel rod and cylinder were held concentrically by a Delryn spacer and lowered into the solution. AC voltage with frequency ω was applied to the capacitor in series with a resistor, R_{in}. Both

TABLE I. Measured and calculated diffusion constants.

Solvent	η (cP)	D_{DMA} (Å^2/ns)	D_{R3B} (Å^2/ns)	D (Å^2/ns) ($D_{DMA}+D_{R3B}$)	Calculated[c] D (Å^2/ns)
acetonitrile	0.341[a]	305	133	438	764
ethanol	1.08[a]	182	59.8	242	242
propylene glycol	49.90	6.7	1.3[b]	8.0	5.2
58/42 propylene glycol/2-butanol	14.70	24.4	4.4[b]	28.8	17.7
23/77 glycerol/2-butanol	14.26	28.3	4.5[b]	32.8	18.3
50/50 ethylene glycol/ethanol	11.97	37.5	7.8	45.3	21.8
41/59 glycerol/ethanol	15.05	19.6	8.6	28.2	17.3

[a]Literature values (Refs. 24, 28).
[b]Calculated values.
[c]Scaled viscosity from measured D for ethanol.

phase and amplitude of V_{in} (across both the capacitor and the resistor) and V_{out} (across the capacitor only) were measured with a digital lock-in amplifier. Capacitance, C, was calculated using the following equation:

$$C = \frac{V_{in}}{V_{out}} \frac{\sin(\phi)}{R_{in}\omega}, \tag{3}$$

where the phase is $\phi = \phi_{out} - \phi_{in}$. For each solvent, measurements were made for two rod/cylinder positions: fully inserted and partially inserted. The two measurements were subtracted to remove end effects. ϵ_{st} is proportional to C. The scaling factor was determined by calibrating the cell using ethanol, for which $\epsilon_{st} = 24.5$.[28] Dielectric constants determined for other pure solvents agree well with literature values. Results are reported in Table II.

III. THEORY

A. Qualitative overview

In all of the electron transfer experiments outlined above, a low concentration of hole donor molecules are surrounded by a higher concentration of hole acceptor molecules. (An electron is transferred from the DMA to the photoexcited R3B.) The donors are far enough apart to be noninteracting, so the theory uses a model in which a single donor molecule is surrounded by a given concentration of acceptor molecules, all diffusing in solution [see Fig. 1(A)].

Figure 1(B) shows the 3-state electron transfer system. The lowest parabola represents the initial system, with all molecules in their respective ground states. Photoexcitation of the donor brings the system into the state represented by the highest parabola. Following photoexcitation, the system either returns to the ground state via fluorescence or goes to the charge transfer state by transferring an electron. Electron transfer occurs through-solvent with a distance-dependent rate constant. Diffusion and solvent structure affect the distribution of donor–acceptor distances at any given time. Together, the rate constant and donor–acceptor distances determine the survival time of the donor's excited state.

The time- and distance-dependence of electron transfer in a given system depends on a wide variety of solute and solvent dependent parameters. For example, individual donor/acceptor molecular properties determine the magni-

TABLE II. Measured solvent parameters.

Solvent	ϵ_{op}	ϵ_{st}	σ (Å)	τ (ns)
acetonitrile	1.7999	35.9[a]	3.62	1.45
ethanol	1.8523	24.5	4.14	2.07
propylene glycol	2.0472	29.2	4.72	2.80
58/42 propylene glycol/2-butanol	2.0073	22.3	4.82[b]	2.66
23/77 glycerol/2-butanol	2.0025	19.3	4.90[b]	2.60
50/50 ethylene glycol/ethanol	1.9631	32.8	4.24[b]	2.21
41/59 glycerol/ethanol	2.0070	31.9	4.50[b]	2.34

[a]Literature values (Ref. 24).
[b]Average diameter of the mixture's components.

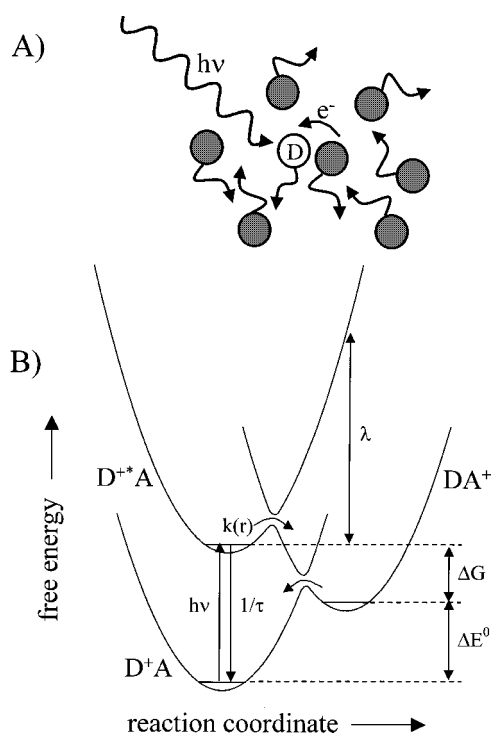

FIG. 1. (A) Hole donor molecule surrounded by diffusing hole acceptors. Following donor excitation, nearby acceptors compete for electron transfer based on the rate constant for transfer at their respective distances. (B) Free energy diagram of 3-state model consisting of (1) donor/acceptor ground state, (2) photoexcited donor/ground state acceptor, and (3) charge transfer state. Excited state population is created by photoexcitation with energy $h\nu$ and removed by fluorescence with lifetime τ and electron transfer with rate $k(r)$. The free energy difference between states 1 and 3 is the difference in donor/acceptor redox potentials, ΔE^0. The free energy difference between states 2 and 3 is ΔG, the free energy associated with electron transfer. λ is the reorganization energy.

tude and distance-dependence of their electronic coupling. The difference in donor/acceptor reduction/oxidation potentials (ΔE^0) and reorganization energy (λ), shown in Fig. 1(B), determine the energetics of the reaction. As the solvent dielectric constant decreases, ΔE^0 increases. A larger difference in donor/acceptor reduction/oxidation potentials leads to a smaller driving force for the electron transfer. Solvent dielectric constants also determine the solvation energies and solvent reorganization energies. In more polar solvents, less energy is required to create charges. In addition, polar solvents screen Coulomb interactions between ions. However, in less polar solvents, a lot of energy can be gained by removing charges from ions, if molecules are initially charged. The effects of polarity depend strongly on the molecular charges of a specific electron transfer system. Even when the donor/acceptor molecules are specified, the distance-dependent rate constant can change significantly with solvent.[1]

The radial distribution function has a significant influence on the distribution of donor–acceptor distances found in an experimental system. Molecules in solution organize to pack in a spatially compact manner. Figure 2(A) shows a schematic of packing in two dimensions. Because of this packing, it is more likely to find two molecules separated by one solvent diameter (σ) than by 1.5 σ. Figure 2(B) shows an example of a solvent radial distribution function, $g(r)$. In general, a solute's density oscillates about the average density in the same manner as the solvent's $g(r)$. Therefore, $g(r)$ is the distribution of donor-acceptor separation distances.[29] This means that the acceptor concentration near contact is significantly greater than the average concentration. Because most electron transfer occurs at very small distances, including the radial distribution function changes the effective acceptor concentration participating in the reaction. The local acceptor concentration, which is controlled by the radial distribution function, has a significant effect on the transfer dynamics.

Diffusion plays a key role in the overall time-dependence of electron transfer in liquids. The rate of diffusion is determined by the solvent structure and the hydrodynamic effect. Diffusion does not occur in an isotropic continuum. It is constrained by the fact that the equilibrium distribution of acceptor molecules must follow the solvent's structure, $g(r)$. As a result, molecular diffusion occurs within a potential of mean force ($-\ln[g(r)]$) rather than freely.[30,31] The effects are strongest within the first solvent shell. In addition, the hydrodynamic effect[32,33] is included in the theory via a distance-dependent diffusion constant, $D(r)$, shown in Fig. 2(C). The consequence of the hydrodynamic effect is slower diffusion at short donor–acceptor distances because there are fewer pathways around intervening molecules that bring the donor and acceptor closer together. The hydrodynamic effect can slow diffusion near contact by a factor of 4 compared to bulk diffusion.[32,33] Because most electron transfer occurs near contact, the radial distribution function and the hydrodynamic effect have a significant influence on the time-dependence of intermolecular electron transfer in a given system.

Figure 3 shows the effects of solvent structure and the

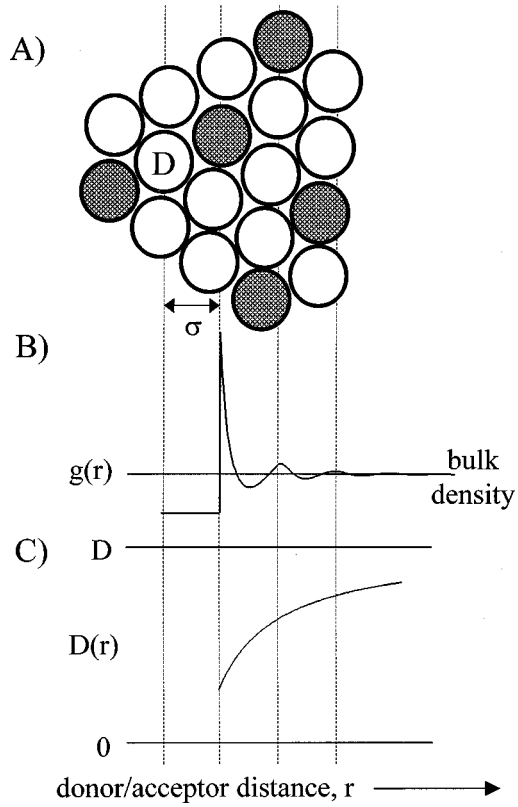

FIG. 2. (A) Example of hard sphere packing in two dimensions. A donor molecule is surrounded by solvent (open) and acceptor (hatched) spheres of diameter σ. (B) A hard sphere radial distribution function, $g(r)$, which shows probability of finding a solute/solvent molecule at a given distance from another molecule in solution (the donor in this case). Molecule density peaks at 1 solvent diameter, σ, dips at 1.5 σ, and approaches the average bulk density by 3 σ. For hard spheres with a packing fraction of 45%, the density at contact is 4.6 times the bulk density. (C) The distance-dependent diffusion constant, $D(r)$, resulting from the hydrodynamic effect for stick boundary conditions. Lines show the limits of no diffusion (0) and the bulk diffusion rate [$D(\infty)=D$]. For the example shown (R3B and DMA, used in the experiments), the contact value of $D(r)$ is 28% of the bulk value.

hydrodynamic effect on excited state survival probability (the probability that the initially excited donor is still excited) as a function of time. The hydrodynamic effect, $D(r)$, makes the decay significantly slower, especially at longer times, by slowing down the diffusion at short distances. $g(r)$ has a much greater effect at shorter times because it increases the effective acceptor concentration at short distances where transfer occurs quickly. The parameters used in Fig. 3 correspond to the best fit parameters for the glycerol/2-butanol mixture (see below). The changes in diffusion are most significant for low viscosity solvents like acetonitrile and ethanol, in which molecules diffuse quickly. The effects of $g(r)$ are strongest in solvents with slow diffusion, in which transfer is dominated by the initial donor-acceptor distance distribution. $g(r)$ plays a more significant role in solvents with larger solvent diameters than those used in this paper. Because $g(r)$ and/or $D(r)$ will have a strong effect in almost any solvent, it is important to include them in electron transfer calculations.

B. Observables

In the systems described here, electron transfer is induced by photoexcitation of the donor molecule. Either fluo-

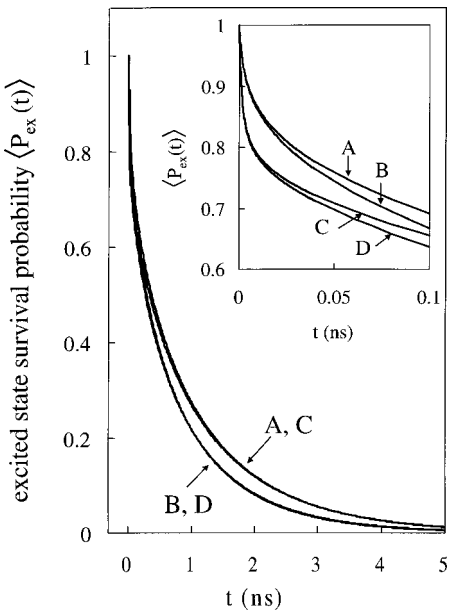

FIG. 3. Unconvolved theoretical excited state survival probability, $\langle P_{ex}(t)\rangle$ vs time showing the effects of including solvent structure, $g(r)$, and the hydrodynamic effect, $D(r)$. (A) Includes $D(r)$; (B) includes neither; (C) includes $D(r)$ and $g(r)$; (D) includes $g(r)$ only. Inset shows short time behavior. Parameters used are for R3B and 0.15 M DMA in glycerol/2-butanol with stick boundary conditions. Electronic coupling parameters are $J_0=320\,\mathrm{cm}^{-1}$ and $\beta=1\,\text{Å}^{-1}$ as shown in Fig. 8. At longer times, $D(r)$ is important, but curves with and without $g(r)$ are indistinguishable. At short times, $g(r)$ plays an important role.

rescence or electron transfer follows excitation. The time dependence of donor fluorescence is an observable that corresponds to the ensemble averaged excited state survival probability as a function of time, $\langle P_{ex}(t)\rangle$. A detailed theory has been developed to calculate $\langle P_{ex}(t)\rangle$ for molecules diffusing freely in solution, including solvent structure and the hydrodynamic effect.[20–23] The final results are given here,

$$\langle P_{ex}(t)\rangle = \exp(-t/\tau) \times \exp\left(-4\pi C\int_{r_m}^{\infty}[1-S_{ex}(t|r_0)]r_0^2 g(r_0)dr_0\right), \tag{4}$$

where τ is the fluorescence lifetime of samples containing no acceptors, C is the acceptor concentration, r is the donor–acceptor center-to-center separation distance, and $g(r)$ is the solvent radial distribution function. The donor/acceptors are assumed to be hard spheres and cannot approach closer than the sum of their radii, r_m. $S_{ex}(t|r_0)$ is the two-particle survival probability. $S_{ex}(t|r_0)$ represents the probability that for a one-donor one-acceptor system in which the donor is photoexcited at $t=0$, the donor is still excited at time t, given that the acceptor was at r_0 at $t=0$. $S_{ex}(t|r_0)$ is the solution to the following equation, and is calculated numerically:

$$\frac{\partial}{\partial t}S_{ex}(t|r_0)=L_{r_0}^{+}S_{ex}(t|r_0)-k(r_0)S_{ex}(t|r_0), \tag{5}$$

where $k(r)$ is the distance-dependent electron transfer rate constant. $L_{r_0}^{+}$ is the adjoint of the Smoluchowski diffusion operator,

$$L_{r_0}^{+}=\frac{1}{r_0^2}\exp(V(r_0))\frac{\partial}{\partial r_0}D(r_0)r_0^2\exp(-V(r_0))\frac{\partial}{\partial r_0}, \tag{6}$$

where $D(r)$ is the distance-dependent diffusion constant, and $V(r)$ is the distance-dependent potential in which the acceptors are diffusing, divided by k_BT.

Another useful observable that we measure is the steady-state fluorescence yield, Φ. It is the ratio of fluorescence from a sample with acceptors to one with no acceptors. The fluorescence yield provides some information on time scales fast compared to the instrument response of the instrument used to make the time dependent fluorescence measurements. In time-dependent measurements, the shortest time scale behavior of the electron transfer is masked by the convolution of the instrument response with the electron transfer dynamics. Φ can be written as the ratio of integrated areas under the unconvolved $\langle P_{ex}(t)\rangle$ curves,

$$\Phi=\frac{\int_0^{\infty}\langle P_{ex}(t)\rangle dt}{\tau}, \tag{7}$$

where the area under $\langle P_{ex}(t)\rangle$ with no acceptors is the fluorescence lifetime, τ. Because the unconvolved probability decays all start at 1 at time $t=0$, the area under a curve is drastically decreased when very fast electron transfer removes population from the excited state very quickly. The sensitivity of fluorescence yield to the unconvolved $\langle P_{ex}(t)\rangle$ decays makes it a valuable tool for studying electron transfer dynamics.

The fraction of transfer that is occurring within the instrument response, ET_{ir}, can be calculated roughly from experimental data,

$$ET_{ir}=1-\frac{1-[\int_0^{\infty}\langle P_{ex}(t)\rangle_{exp}dt/\tau]}{1-\Phi_{exp}}, \tag{8}$$

where $\langle P_{ex}(t)\rangle_{exp}$ is the experimental, convolved $\langle P_{ex}(t)\rangle$ scaled to 1 at its peak, and Φ_{exp} is the experimental fluorescence yield.

C. Rate constant

$\langle P_{ex}(t)\rangle$ can be calculated with any distance-dependent form of the electron transfer rate constant, $k(r)$. For electron transfer in the normal region ($-\Delta G<\lambda$), a widely used form of $k(r)$ was developed by Marcus,[34–39]

$$k(r)=\frac{2\pi}{\hbar\sqrt{4\pi\lambda(r)k_BT}}J_0^2\exp\left(\frac{-(\Delta G(r)+\lambda(r))^2}{4\lambda(r)k_BT}\right) \times\exp(-\beta(r-r_m)), \tag{9}$$

where $\hbar$ is Planck's constant divided by 2π, λ is reorganization energy, k_B is Boltzmann's constant, T is temperature, and ΔG is the free energy of electron transfer. The donor–acceptor electronic coupling is characterized by J_0, the magnitude of coupling at contact, and β, which reflects the exponential distance-dependence of the coupling.

ΔG, designated in Fig. 1(B), is the free energy change associated with forward electron transfer. The standard expression for ΔG was developed by Rehm and Weller,[40] and includes excitation energy, redox potentials, and Coulomb

interactions. For the donor/acceptor system used in this paper, there are no Coulomb interactions, so ΔG is not distance-dependent,

$$\Delta G = \Delta E^0 - h\nu, \tag{10}$$

where ΔE^0 is the difference between donor/acceptor reduction/oxidation potentials, given by Eq. (1). $h\nu$ is the donor singlet excited state energy, taken to be the energy at which normalized absorption and fluorescence spectra cross.[39]

The reorganization energy, λ, shown in Fig. 1(B), is the free energy change that would be required to reorient atoms and molecules as if they were forming and solvating the product state, but without actually transferring an electron. λ includes an inner sphere portion, λ_i, and an outer sphere portion, λ_0,[37]

$$\lambda = \lambda_i + \lambda_0, \tag{11}$$

where λ_i includes intramolecular structural changes associated with addition/removal of an electron from the donor/acceptor, and λ_0 includes solvent reorientation about the products. Inner sphere reorganization energies can be calculated,[37,41] and measured.[42,43] In general, $\lambda_0 \gg \lambda_i$, and λ_i has no distance dependence. Therefore, for the experiments described in this paper, which involve the distance dependence of electron transfer, λ_i has only a small effect on the results. The value of λ_i used in the calculations is discussed below. The expression for λ_0 was derived by Marcus,[34–37]

$$\lambda_0(r) = \frac{e^2}{4\pi\epsilon_0}\left(\frac{1}{\epsilon_{op}} - \frac{1}{\epsilon_{st}}\right)\left(\frac{1}{r_d} + \frac{1}{r_a} - \frac{2}{r}\right), \tag{12}$$

where ϵ_{op} and ϵ_{st} are optical and static dielectric constants.

D. Solvent structure

Intermolecular electron transfer in liquids is influenced by the local structure present in condensed-phase solutions.[4,5,20] For hard spheres of diameter σ, the density oscillates about the average density of 1, with a peak at σ, dip at 1.5 σ, and so forth, damped to the average density after ~3 solvent shells [see Fig. 2(B)]. When solute molecules are in solution at low concentration (less than a few tenths molar), they follow the solvent density variation to a reasonable approximation.[29] This means that acceptor molecules follow the solvent radial distribution function about donor molecules. As a result, effective acceptor concentrations about donor molecules are 4.6 times larger than the bulk concentration in the first solvent shell (for 45% packing fraction). In addition, $g(r)$ affects diffusion by restricting molecular motion in order to maintain the solvent structure. For the experimental system in this paper, there are no Coulomb interactions, but diffusion occurs within the potential of mean force,[30,31]

$$V(r) = -\ln[g(r)]. \tag{13}$$

For this work, hard-sphere radial distribution functions are calculated by solving the Percus–Yevick equation[29,44–47] using an algorithm given by Smith and Henderson.[48] The final result is modified by a Verlet–Weis correction.[49]

Solvent diameters (σ) are used to determine the frequency of oscillation. A packing fraction of 45% was used because molecular dynamic simulations predict values between 43% and 48% for dense, room-temperature liquids.[29,49–52] r is the donor/acceptor center-to-center separation distance, so all radial distribution functions are shifted so that the first peak is at the sum of donor/acceptor radii.

E. Hydrodynamic effect

A distance-dependent diffusion constant accounts for the hydrodynamic effect, in which molecules diffuse toward each other slower at short distances because intervening molecules can hinder diffusion toward each other.[30–32,53] One distance-dependent equation for diffusion was developed by Deutsch and Felderhof,[32,33]

$$D(r) = D\left[1 - \frac{3r_d r_a}{r(r_d + r_a)}\right], \tag{14}$$

where D is the sum of the measured donor/acceptor bulk diffusion coefficients. The equation is for stick boundary conditions, which are most appropriate when solute molecules are larger than the solvent molecules.[30] Stick boundary conditions are reasonable for R3B in the small alcohol solvents used in this paper. DMA is also larger than all of the solvents used. A plot of $D(r)$ calculated using Eq. (14) for R3B and DMA is shown in Fig. 2(C). Some calculations have been performed for comparison using the expression developed by Northrup and Hynes for slip boundary conditions,[31]

$$D(r) = D\left[1 - \frac{1}{2}\exp\left(\frac{r_m - r}{\sigma}\right)\right], \tag{15}$$

where r_m is the donor–acceptor contact distance, and σ is the solvent diameter. Slip boundary conditions are most appropriate when solute and solvent molecules are similar sizes.[30]

IV. DATA ANALYSIS

Fluorescence up-conversion and fluorescence yield data were fit simultaneously. $\langle P_{ex}(t)\rangle$ is determined by numerical integration of Eq. (4), which requires knowledge of $S_{ex}(t|r_0)$. $S_{ex}(t|r_0)$ is the numerical solution, determined by partial differencing, of Eq. (5) in conjunction with Eqs. (6), (13), and (14). $\langle P_{ex}(t)\rangle$ is convolved with the instrument response for comparison with fluorescence time decays. Fluorescence yield is calculated according to Eq. (7) by numerically integrating the unconvolved $\langle P_{ex}(t)\rangle$. Calculations were performed using the Marcus distance-dependent rate constant given in Eq. (9) in conjunction with Eqs. (1) and (10)–(12).

Measured bulk diffusion constants (D) can be found in Table I. Measured values for fluorescence lifetimes (τ) and dielectric constants (ϵ_{op} and ϵ_{st}) are reported in Table II. Solvent diameters (σ) were determined by making molecular models of each solvent molecule. Diameters reported in Table II are the diameters of a spherical volume with the same volume as the molecular models. For solvent mixtures, the average diameter of the two solvents was used. R3B and DMA radii of 4.12 Å and 2.75 Å, respectively, were deter-

mined in the same manner. These radii are different than those used in previous experiments.[8] However, we believe that the new method is more accurate.

Inner sphere reorganization energy is assumed to be $\lambda_i = 0.10$ eV. Calculations of λ_i for large, aromatic organic molecules like Rhodamine 3B yield approximately 0.05 eV.[41] This number has been multiplied by 2 to account for donor and acceptor reorganization. Liu *et al.* reported $\lambda_i = 0.2$ eV for a bonded organic donor/acceptor pair.[42] Markel *et al.* measured $\lambda_i = 0.43$ eV in an organic charge transfer complex.[43] However, approximately 1/3 of this was attributed to an intermolecular stretching mode. $\lambda_i = 0.10$ eV seems to be a reasonable approximation for the donor/acceptor considered here.[54] The effects of λ_i will be discussed below.

When the appropriate parameters are used for each solvent, calculations yield $\Delta G = -0.57 - -0.59$ eV and $\lambda = 1.12 - 1.30$ eV at contact. This is within the normal region of electron transfer ($-\Delta G < \lambda$), as depicted in Fig. 1(B), and justifies the use of Eq. (9) as the rate constant.[39]

The distance-dependence of electronic coupling, β, is assumed to be 1 Å^{-1} for all fits unless otherwise specified, because $\beta \sim 1$ Å^{-1} has been reported for most electron transfer experiments in liquids.[13,37,55–57] The assumption was checked by making changes in β (see below). By assuming this value of β, the data fitting process is left with a single adjustable parameter.

V. RESULTS

Figures 4–10 show both time dependent fluorescence up-conversion data and fluorescence yield data taken in all seven solvents. Attempts to fit the data with a simple theory that includes no solvent structure, no hydrodynamic effect, and transfer only at contact were unsuccessful. It was impossible to fit both the fluorescence yield and time decays with a contact-only model, even if solvent structure, $g(r)$, and the hydrodynamic effect, $D(r)$, were included. In addition to a distance-dependent rate constant, $g(r)$ and $D(r)$ are essential to fitting this data correctly. When these effects are not included, only two of the seven data sets can be fit. For those data sets that can be fit, the resulting J_0 values change by a factor of 2–3 when $g(r)$ and $D(r)$ are removed. *When $k(r)$, $D(r)$, and $g(r)$ are included, and all measured and calculated parameters were incorporated as described above, both up-conversion and yield experiments were successfully fit for all seven solvents with a single variable parameter, J_0.* Fits shown in the figures, which include solvent structure and the hydrodynamic effect with stick boundary conditions, were determined with all parameters fixed except J_0. The values for the best fits to J_0 are designated in each figure.

For each solvent, the amount of transfer occurring within the instrument response can be determined roughly using Eq. (8). Less transfer occurs within the instrument response for higher acceptor concentrations and in solvents with higher diffusion constants. For an acceptor concentration of 0.1 M, ~10% of transfer occurs within the instrument response for acetonitrile and ethanol, ~20% for ethylene glycol/ethanol, ~30% for the three more viscous mixtures, and 45% for propylene glycol. Thus, the time dependent data represents a significant portion of the dynamics but it is not complete. The fluorescence yield data provides some information on the short time behavior of the dynamics that is masked by the instrument response.

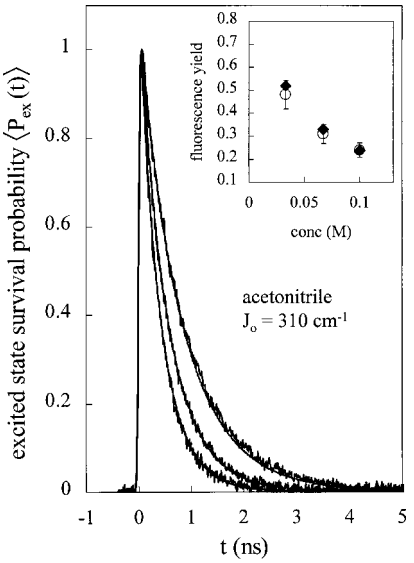

FIG. 4. Data and fits for R3B and 3 DMA concentrations (0.033, 0.067, and 0.100 M) in acetonitrile. $J_0 = 310$ cm^{-1}, $\beta = 1$ Å^{-1} and all other parameters are fixed. Inset shows fluorescence yield data (○) and fits (◆).

Table I lists diffusion constants, D, that are calculated by assuming that D scales linearly with viscosity. The measured D for ethanol was multiplied by a ratio of viscosities to determine these values. Clearly, the experimental diffusion constants do not simply follow solvent viscosity. Diffusion is much faster in the solvent mixtures than would be expected from a linear viscosity dependence.

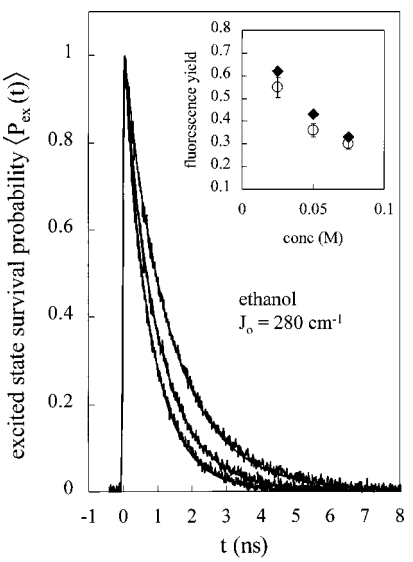

FIG. 5. Data and fits for R3B and 3 DMA concentrations (0.025, 0.050, 0.075 M) in ethanol. $J_0 = 280$ cm^{-1}, $\beta = 1$ Å^{-1} and all other parameters are fixed. Inset shows fluorescence yield data (○) and fits (◆).

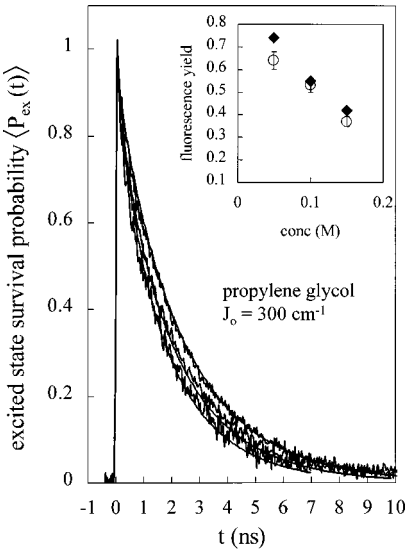

FIG. 6. Data and fits for R3B and 3 DMA concentrations (0.050, 0.100, and 0.150 M) in propylene glycol. $J_0 = 300\ cm^{-1}$, $\beta = 1\ Å^{-1}$ and all other parameters are fixed. Inset shows fluorescence yield data (○) and fits (◆).

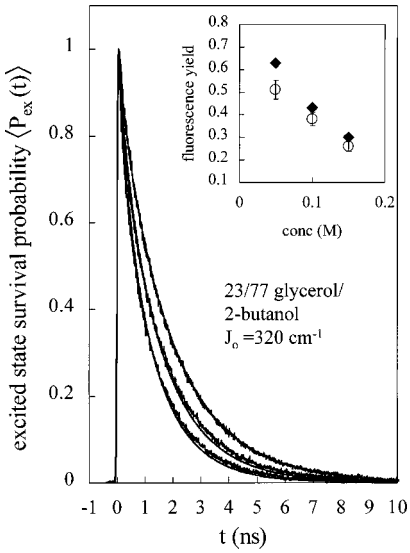

FIG. 8. Data and fits for R3B and 3 DMA concentrations (0.050, 0.100, and 0.150 M) in 23/77 v/v glycerol/2-butanol. $J_0 = 320\ cm^{-1}$, $\beta = 1\ Å^{-1}$, and all other parameters are fixed. Inset shows fluorescence yield data (○) and fits (◆).

VI. DISCUSSION

Figures 4–10 show fits to steady state and time-dependent data using $k(r)$, $D(r)$, and $g(r)$, with J_0 as the only fitting parameter. J_0 values are reported in Table III. The ability of the theory to do a good job of fitting the shape and concentration dependence of data in all seven solvents is remarkable considering that the solvents include acetonitrile, pure hydrogen bonding liquids, and hydrogen bonding solvent mixtures. From one solvent to another, there is a wide variation in the input parameters for the calculations, reflecting the variation in the physical properties of the systems.

In addition to being able to fit each data set by fixing all parameters except J_0, the fits result in very consistent J_0 values (see Table III). The magnitude of the electronic coupling matrix element, J_0, is expected to be similar for the same donor/acceptor pair in different solvents. For the first five solvents (see Figs. 4–8), acetonitrile, ethanol, propylene glycol, propylene glycol/2-butanol, and glycerol/2-butanol, all of the J_0 values are $300 \pm 20\ cm^{-1}$. The J_0's measured in the solvents ethylene glycol/ethanol and glycerol/ethanol (see Figs. 9 and 10) are 540 cm^{-1} and 660 cm^{-1}, respectively. In these mixtures, more than 1/3 of the solvent molecules have an OH for every carbon atom. In addition, 73%–76% of the solvent carbon atoms have attached OH groups. Although the J_0 values are somewhat higher, they are nonetheless in reasonable overall agreement. In all cases, the shapes of the time-dependent curves, the yield data, and the

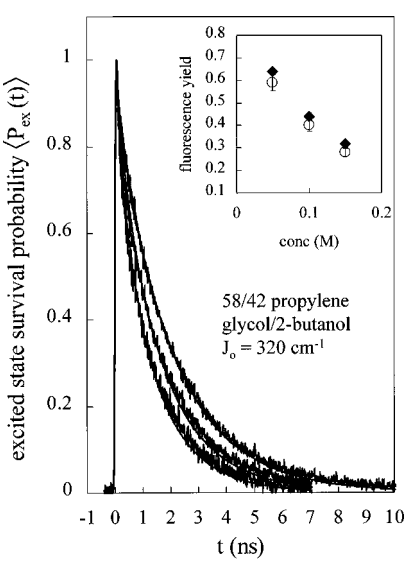

FIG. 7. Data and fits for R3B and 3 DMA concentrations (0.050, 0.100, and 0.150 M) in 58/42 v/v propylene glycol/2-butanol. $J_0 = 320\ cm^{-1}$, $\beta = 1\ Å^{-1}$ and all other parameters are fixed. Inset shows fluorescence yield data (○) and fits (◆).

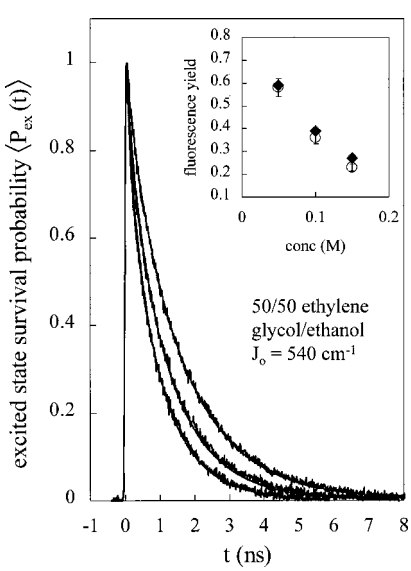

FIG. 9. Data and fits for R3B and 3 DMA concentrations (0.050, 0.100, and 0.150 M) in 50/50 v/v ethylene glycol/ethanol. $J_0 = 540\ cm^{-1}$, $\beta = 1\ Å^{-1}$, and all other parameters are fixed. Inset shows fluorescence yield data (○) and fits (◆).

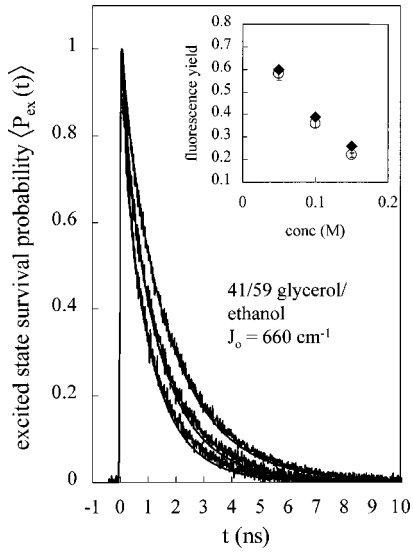

FIG. 10. Data and fits for R3B and 3 DMA concentrations (0.050, 0.100, and 0.150 M) in 41/59 v/v glycerol/ethanol. $J_0=660\ \mathrm{cm}^{-1}$, $\beta=1\ \text{Å}^{-1}$, and all other parameters are fixed. Inset shows fluorescence yield data (○) and fits (◆).

concentration dependence can be fit with a single adjustable parameter in seven solvents and the values of J_0 obtained are in reasonable accord. For each solvent, a range of J_0 values that has maximum and minimum values differing by ~20% gives acceptable fits to both the time and the yield data.

These fits were performed with the hydrodynamic effect included, using stick boundary conditions [Eq. (14)]. For comparison, the data were also fit using slip boundary conditions [Eq. (15)]. The resulting J_0 values are shown in Table III, column 3. Using slip boundary conditions produces noticeably worse fits than using stick boundary conditions. In addition, the resulting J_0 values show considerable inconsistency. Given the results of the fits with slip boundary conditions and the relative sizes of the solute and solvents, stick boundary conditions appear to be appropriate.

The inner sphere reorganization energy, λ_i, has an effect on the J_0 values. However, because λ_i is not distance-dependent and is small enough compared to λ_0, it essentially does not affect the distance-dependence of the rate constant [Eq. (9)]. Therefore, it does not affect our ability to fit the data, and only affects fits by changing the resulting value of J_0. For acetonitrile, λ_i values of 0.00, 0.10, and 0.20 eV result in $J_0=200$, 310, and 480 cm^{-1}. These values of λ_i are in the expected range for organic substrates.[41–43,54] Because λ_i has not been calculated for the molecules in this experimental system specifically, we cannot know J_0 exactly. However, because λ_i is not solvent-dependent, changing λ_i changes J_0 by virtually the same factor in all of the solvents under consideration, and does not affect the consistency of J_0 values.

The two mixtures with solvent components containing an OH on each carbon yield larger values of J_0 from the fits than the five other mixtures. The possibility that errors in the values of D are responsible for the larger values of J_0 was tested. Table III shows that if slip boundary conditions are used, ethylene glycol/ethanol can be fit with $J_0=320\ \mathrm{cm}^{-1}$. However, slip boundary conditions do not make it possible to fit glycerol/ethanol data with J_0 near 300 cm^{-1}. Using slip boundary conditions does not resolve the discrepancy in J_0 values. Table III also shows the results of calculations in which D was varied to obtain $J_0=300\ \mathrm{cm}^{-1}$. The fourth column in the table shows the percent change in D from its measured value required to obtain $J_0=300\ \mathrm{cm}^{-1}$ for each solvent. For the first five solvents, little or no variation is required. However, for ethylene glycol/ethanol, a 50% change in D was required. This value is definitely not within the experimental error of measured D values. For glycerol/ethanol, it was simply not possible to fit the data with $J_0=300\ \mathrm{cm}^{-1}$ regardless of the value of D chosen.

Another possible explanation for the variation in J_0 for two of the solvents is that β varies substantially with solvent. The data were fit allowing β to vary using $J_0=300\ \mathrm{cm}^{-1}$ as the target (see Table III, column 5). For the first five solvents, β values are within the range $\sim 0.95\ \text{Å}^{-1} \leqslant \beta \leqslant \sim 1.05\ \text{Å}^{-1}$, a range that is reasonable for electron transfer in liquids.[13,37,55–57] The small variation in β should not be taken as a measurement of the variation of β with solvent. Given the uncertainty of other input parameters, these are all essentially equivalent. However, data taken in ethylene glycol/ethanol and glycerol/ethanol require $\beta=0.7$ to obtain $J_0=300\ \mathrm{cm}^{-1}$. This is small value of β, and is probably outside the range of reasonable values, of more significance, β would not be expected to change this much within a group of polar liquids.

The net result is that the electron transfer data in five of

TABLE III. Fitting results.

Solvent	J_0 (cm^{-1}) one-parameter fit	J_0 (cm^{-1}) with slip boundary	% change D to obtain $J_0=300\ \mathrm{cm}^{-1}$	β (Å^{-1}) to obtain $J_0=300\ \mathrm{cm}^{-1}$
acetonitrile	310	140	0	0.95
ethanol	280	100	−2	1.06
propylene glycol	300	220[a]	0	1.0
58/42 propylene glycol/2-butanol	320	210[a]	−1	0.96
23/77 glycerol/2-butanol	320	150[b]	−2	0.94
50/50 ethylene glycol/ethanol	540	320[b]	50[b]	0.73
41/59 glycerol/ethanol	660	420[b]	N/A[c]	0.70

[a]Worse quality fit than single parameter fit to J_0.
[b]Significantly worse quality fit than single parameter fit to J_0.
[c]It is not possible to fit both time and yield data with $J_0=300\ \mathrm{cm}^{-1}$ by changing D.

the solvents show completely consistent agreement with the theoretical calculations. Using the measured and calculated input parameters, $J_0 = 300\,\mathrm{cm}^{-1}$ and $\beta = 1\,\text{Å}^{-1}$. Varying these parameters outside of a narrow range is inconsistent with the data. The two solvents that contain more substantial numbers of OH groups per solvent carbon can also be fit, but require larger values of J_0. We believe that this discrepancy arises from the model used to describe the radial distribution function of the acceptors about the donors in solvents in which more than 1/3 of the molecules have an OH substituent on each carbon atom. The model has the solutes tracking the radial distribution function of the solvent.[29] In a subsequent publication,[58] electron transfer of the donor/acceptor system studied here but in pure ethylene glycol solvent will be addressed. It will be shown that it is necessary to substantially modify both the radial distribution function and the hydrodynamic effect in a consistent manner to describe the electron transfer data. Small remnants of the effects observed in pure ethylene glycol appear to exist in mixtures containing ethylene glycol or glycerol. It is interesting to note that the electron transfer dynamics in pure propylene glycol are described well using the standard model of the solute radial distribution function.

Another interesting trend to note is that the calculations somewhat overestimate the fluorescence yields. It is not possible to get better fits to the yields and simultaneously obtain acceptable fits to the time decays. The fact that the calculations overestimate the fluorescence yields means that the electron transfer dynamics are systematically faster at very short times (shorter than the pulse duration) than predicted by the calculations. Small problems in accounting for very fast transfer can lead to large errors in the yield calculations because, as noted in the Results, some samples experience up to 45% of their electron transfer within the instrument response. One possible reason for the discrepancy at short times may be the hard sphere form of $g(r)$. A hard sphere $g(r)$ has a sharp cut-off at the sum of the donor/acceptor radii. A hard sphere $g(r)$ does a good job of accounting for the local concentration in the first solvent shell,[5] but it is not a precise description of the spatial separations of the donor and acceptors in the first solvent shell. The ability of a donor and acceptor to come closer together than the hard sphere cut-off could enhance the very short time transfer rate. Another possibility is that using an exponential decay of the electronic coupling is not adequate at very short distance. Details of the molecular wavefunctions may become important. In addition, molecular orientation has not been considered in these calculations. Model calculations show that the influence of orientation on electron transfer dynamics is washed out when the dynamics are averaged over orientation and distance.[59] However, the very short time dynamics are dominated by the subensemble of donor/acceptor molecules that are essentially in contact. For this subensemble, the exact form of the wavefunctions and orientational effects may come into play. The fluorescence yield indicates that a full description of the dynamics at very short time is not in hand. Future experiments with fs resolution will be used to address the very short time behavior of the systems studied here.

VII. CONCLUDING REMARKS

Photoinduced electron transfer in liquid solution is a complex process affected by numerous factors. In this paper, time resolved fluorescence and fluorescence yield experiments examining the donor/acceptor electron transfer dynamics in seven liquids were presented. The theory employed to analyze the data includes all of the important aspects of electron transfer in solution. Through measurement or calculation of all the necessary input parameters, only the fundamental electronic coupling parameters were left as unknowns. It was impossible to obtain reasonable fits to the data with a simpler theory that does not include a distance-dependent rate constant, solvent structure, and the hydrodynamic effect.

When all the details were included, fits performed with only one adjustable parameter (J_0, the magnitude of the electron transfer coupling matrix element at donor/accepter contact) were successful for all seven solvents. J_0 values, which should depend on donor/acceptor identity and should not be influenced greatly by the solvent properties, are in complete agreement for five of the solvents. For two of the solvents that are mixtures with ethylene glycol and glycerol as one of the components, the J_0 values are somewhat larger than in the other solvents. In a subsequent paper, it will be suggested that solvent molecules with an OH on each carbon atom can modify the solutes' radial distribution functions and the hydrodynamic effect.[58] Since the radial distribution function and the hydrodynamic effect can play an important role in electron transfer dynamics in solution, reasonably accurate knowledge of the spatial distributions of solutes in a given solvent is necessary to have an accurate description of electron transfer dynamics. The results presented here show that in many solvents, even hydrogen bonding solvents and mixtures, standard, simple assumptions about solute spatial distributions in solvents are adequate.

In these experiments, forward electron transfer was studied. Since the time dependent populations of the species following charge transfer depend on the details of electron back transfer, future experiments will study geminate recombination. The theory employed here to describe forward transfer has also been developed to describe geminate recombination.[22,60–62] The theory of geminate recombination includes all of the important physical features that are used to describe the forward transfer. The coupled problems of forward transfer and geminate recombination are complex. Experiments on faster time scales and examining geminate recombination will provide increased understanding of electron transfer in liquid solution.

ACKNOWLEDGMENTS

The authors would like to thank Professor Robert L. Kay, Carnegie Mellon University, for help developing a method to measure solution capacitance; and Professors Hans C. Andersen and Vijay Pande, Stanford University, for useful discussions on structure in hydrogen bonding solvents. We would like to thank Kristin Weidemaier, Tom Treynor, and An-tung Anthony Liu for help performing preliminary experiments on this project; Ambika Shankar for

help with sample preparation and data collection; Koichiro Shirota and Alexandre Kretchetov for help developing equations for the capacitance measurements; and Shelley Minteer for suggesting cyclic voltammetry as a diffusion measurement technique. This research was supported by the Department of Energy, Office of Basic Energy Sciences (Grant No. DE-FG03-84ER13251).

[1] H. L. Tavernier, A. V. Barzykin, M. Tachiya, and M. D. Fayer, J. Phys. Chem. B **102**, 6078 (1998).
[2] H. L. Tavernier and M. D. Fayer, J. Phys. Chem. (to be published).
[3] Y. P. Liu and M. D. Newton, J. Phys. Chem. **98**, 7162 (1994).
[4] K. Weidemaier, H. L. Tavernier, S. F. Swallen, and M. D. Fayer, J. Phys. Chem. A **101**, 1887 (1997).
[5] S. F. Swallen, K. Weidemaier, H. L. Tavernier, and M. D. Fayer, J. Phys. Chem. **100**, 8106 (1996).
[6] L. Burel, M. Mostafavi, S. Murata, and M. Tachiya, J. Phys. Chem. A **103**, 5882 (1999).
[7] S. Iwai, S. Murata, and M. Tachiya, J. Chem. Phys. **109**, 5963 (1998).
[8] K. Weidemaier, H. L. Tavernier, and M. D. Fayer, J. Phys. Chem. B **101**, 9352 (1997).
[9] H. Aota, S. Araki, Y. Morishima, and M. Kamachi, Macromolecules **30**, 4090 (1997).
[10] C. D. Borsarelli, J. J. Cosa, and C. M. Previtali, Photochem. Photobiol. **68**, 438 (1998).
[11] J. W. I. Hackett and C. Turro, J. Phys. Chem. A **102**, 5728 (1998).
[12] L. Hammarström, T. Norrby, G. Stenhagen, J. Martensson, B. Akermark, and M. Almgren, J. Phys. Chem. B **101**, 7494 (1997).
[13] H. B. Gray and J. R. Winkler, Annu. Rev. Biochem. **65**, 537 (1996).
[14] Y. Z. Hu, S. Tsukiji, S. Shinkai, S. Oishi, and I. Hamachi, J. Am. Chem. Soc. **122**, 241 (2000).
[15] A. J. DiBilio, C. Dennison, H. B. Gray, B. E. Ramirez, A. G. Sykes, and J. R. Winkler, J. Am. Chem. Soc. **120**, 7551 (1998).
[16] F. D. Lewis, T. Wu, Y. Zhang, R. L. Letsinger, S. R. Greenfield, and M. R. Wasielewski, Science **277**, 673 (1997).
[17] A. M. Brun and A. Harriman, J. Am. Chem. Soc. **114**, 3656 (1992).
[18] P. J. Dandliker, M. E. Nunez, and J. K. Barton, Biochemistry **37**, 6491 (1998).
[19] S. O. Kelley and J. K. Barton, Science **283**, 375 (1999).
[20] S. F. Swallen, K. Weidemaier, and M. D. Fayer, J. Chem. Phys. **104**, 2976 (1996).
[21] M. Tachiya, Radiat. Phys. Chem. **21**, 167 (1983).
[22] Y. Lin, R. C. Dorfman, and M. D. Fayer, J. Chem. Phys. **90**, 159 (1989).
[23] R. C. Dorfman, Y. Lin, and M. D. Fayer, J. Phys. Chem. **94**, 8007 (1990).
[24] J. A. Riddick, W. B. Bunger, and T. K. Sakano, *Organic Solvents: Physical Properties and Methods of Purification*, 4th ed. (Wiley, New York, 1986).
[25] A. Weller, Z. Phys. Chem., Neue Folge **133**, 93 (1982).
[26] T. Yamazaki, I. Yamazaki, and A. Osuka, J. Phys. Chem. B **102**, 7858 (1998).
[27] J. E. Baur and R. M. Wightman, J. Electroanal. Chem. **305**, 73 (1991).
[28] J. A. Riddick and W. B. Bunger, *Organic Solvents: Physical Properties and Methods of Purification*, 3rd ed. (Wiley, New York, 1970).
[29] G. J. Throop and R. J. Bearman, J. Chem. Phys. **42**, 2408 (1965).
[30] S. A. Rice, *Diffusion-Limited Reactions* (Elsevier, Amsterdam, 1985).
[31] S. H. Northrup and J. T. Hynes, J. Chem. Phys. **71**, 871 (1979).
[32] J. M. Deutch and B. U. Felderhof, J. Chem. Phys. **59**, 1669 (1973).
[33] R. Zwanzig, Adv. Chem. Phys. **15**, 325 (1969).
[34] R. A. Marcus, J. Chem. Phys. **24**, 966 (1956).
[35] R. A. Marcus, J. Chem. Phys. **24**, 979 (1956).
[36] R. A. Marcus, Annu. Rev. Phys. Chem. **15**, 155 (1964).
[37] R. A. Marcus and N. Sutin, Biochim. Biophys. Acta **811**, 265 (1985).
[38] N. Sutin, in *Electron Transfer in Inorganic, Organic, and Biological Systems*, edited by J. R. Bolton, N. Mataga, and G. McLendon (The American Chemical Society, Washington, 1991), pp. 25–43.
[39] J. R. Bolton and M. D. Archer, in *Electron Transfer in Inorganic, Organic, and Biological Systems*, edited by J. R. Bolton, N. Mataga, and G. McLendon (The American Chemical Society, Washington, 1991), pp. 7–23.
[40] D. Rehm and A. Weller, Isr. J. Chem. **8**, 259 (1970).
[41] J. M. Hale, in *Reactions of Molecules at Electrodes*, edited by N. S. Hush (Wiley–Interscience, New York, 1971), pp. 229–257.
[42] J. Y. Liu and J. R. Bolton, J. Phys. Chem. **96**, 1718 (1992).
[43] F. Markel, N. S. Ferris, I. R. Gould, and A. B. Myers, J. Am. Chem. Soc. **114**, 6208 (1992).
[44] J. K. Percus, Phys. Rev. Lett. **8**, 462 (1962).
[45] E. Thiele, J. Chem. Phys. **39**, 474 (1963).
[46] M. S. Wertheim, Phys. Rev. Lett. **10**, 321 (1963).
[47] J. K. Percus and G. Y. Yevick, Phys. Rev. **120**, 1 (1958).
[48] W. R. Smith and D. Henderson, Mol. Phys. **19**, 411 (1970).
[49] L. Verlet and J. J. Weis, Phys. Rev. A **5**, 939 (1972).
[50] J. P. Hansen and I. R. McDonald, *Theory of Simple Liquids* (Academic, London, 1976).
[51] D. A. McQuarrie, *Statistical Mechanics* (Harper & Row, New York, 1976).
[52] H. C. Andersen (private communication).
[53] P. G. Wolynes and J. M. Deutch, J. Chem. Phys. **65**, 450 (1976).
[54] M. Chanon, M. D. Hawley, and M. A. Fox, in *Photoinduced Electron Transfer. Part A: Conceptual Basis*, edited by M. A. Fox and M. Chanon (Elsevier, New York, 1988), pp. 1–60.
[55] G. L. Closs and J. R. Miller, Science **240**, 440 (1988).
[56] J. R. Miller, J. V. Beitz, and R. K. Huddleston, J. Am. Chem. Soc. **106**, 5057 (1984).
[57] T. Guarr and G. McLendon, Coord. Chem. Rev. **68**, 1 (1985).
[58] H. L. Tavernier and M. D. Fayer, J. Chem. Phys. (submitted).
[59] R. P. Domingue and M. D. Fayer, J. Chem. Phys. **83**, 2242 (1985).
[60] R. C. Dorfman and M. D. Fayer, J. Chem. Phys. **96**, 7410 (1992).
[61] A. I. Burshtein, Chem. Phys. Lett. **194**, 247 (1992).
[62] A. I. Burshtein, A. A. Zharikov, and N. V. Shokhirev, J. Chem. Phys. **96**, 1951 (1992).